Journal of Sustainable Construction Materials and Technologies
Web page info: https://jscmt.yildiz.edu.tr
DOI: 10.47481/jscmt.1165940

JSCMT
Journal of Sustainable Construction
Materials and Technologies

Research Article

Influence of porosity on the free vibration response of sandwich functionally graded porous beams

Sura Kareem Abbas AL-ITBI[*] , **Ahmad Reshad NOORI**

Department of Civil Engineering, İstanbul Gelişim University, İstanbul, Türkiye

ARTICLE INFO

ABSTRACT

Functionally graded materials are composite materials used to build a variety of structures. The porosity made in these materials may negatively affect some behavior aspects like stiffness and strength, but it may provide superior performance in other fields like vibration reduction, thermal isolation, energy absorption, and others. In this paper, we will discuss the effect of porosity on the natural frequencies for functionally graded porous (FGP) sandwich beams. The mechanical properties of the FGP sandwich beams change with the thickness direction's porosity. The free vibration of the beams is examined with the effect of porosity. The analysis is carried out for four different beam supporting types (hinged – hinged, fixed – fixed, free, fixed – hinged). Various porosity ratios are considered with a range from (0.1–0.9). Forty–four samples are analyzed for each type of core material distribution which is the symmetric material constitutive relationships (SMCR) and uniform core material. The results gained from the analysis show that the porosity constant has a significant effect on the natural frequencies of the FGP sandwich beams.

Cite this article as: Al-Itbi, SKA., & Noori, AR. (2022). Influence of porosity on the free vibration response of sandwich functionally graded porous beams. *J Sustain Const Mater Technol*, 7(4), 291–301.

1. INTRODUCTION

Engineering designers are aimed to provide superior structure performance regards various aspects. The structure needs to withstand applied loads in additional requirements that need to be met. Users and designer requirements are continuously developed so that conventional materials cannot give acceptable performance. Damping, strength, stiffness, thermal isolation, lightweight, environmental needs, vibration characteristics, and many more properties may not be met with different materials. For this reason, functionally graded materials (FGMs) should be preferred. Although

fabrication technology of FGMs is beginning, they provide various benefits such as high stiffness, lightweight, and thermal isolation. A positive relationship between cross section thickness and natural frequency is explored, in which the beam's maximum frequency can be detected [1]. Functionally graded materials are composite materials that may contain two or more different materials. Cellular materials can be divided into two categories depending on the porosity framework: open or closed cells. In closed cell core type, the porous cannot be interconnected in counter to open cell type. Each type has specific performance and characteristics that give the engineers various choices and solutions [2].

*Corresponding author.
*E-mail address: surak985@gmail.com

An efficient approach was introduced by [3] to describe the behavior of (SMCR) and monotonic material constitutive relationships (MMCR), which is two types of functionally graded sandwich beams. It reveals a positive relationship between frequency and porosity value in SMCR and MMCR models. It was concluded that the periods of vibration and amplitude are higher when the beam material is MMCR compared with SMCR. When the MMCR porosity modulus rises, more intense vibrations can be predicted. The SMCR material provides the lowest deflection and the highest natural frequencies.

A unified analytical model was established in [4] to study the vibration behavior of functionally graded deep porous beams (straight and curved). The first-order beam theory was used in the formula. The response of forced vibration for FG beams was examined by [5], with the porosity changing in the thickness direction. It was also mentioned that to obtain realistic models, a solid planar continuity model should be used in modeling deep beams. The vibration was categorized depending on vibration characteristics into various categories by [6]. Core materials can alternatively be made of open and closed cell metal foam. Thermoset polymers (unsaturated polyesters, epoxies, etc.) or thermoset polymers (laminates of glass or carbon fiber reinforced thermoplastics) are frequently used as face materials. In rare circumstances, sheet metal is also utilized as a skin material where core and skins are merged [7]. Under various core configurations and core materials, the sandwich beam structure's inherent frequencies and mode shapes were determined by [8]. A finite element (FE) approach was applied to examine the beam.

Ritz approach was used in conjunction with a four-direct iterative algorithm by [9]. The performances of the beam with various porosity distributions were contrasted. In contrast, two non-uniform functionally graded porosity distributions and a uniform distribution were considered. The impacts of the porosity coefficient, slenderness ratio, and thickness ratio were thoroughly examined using numerical data. Porosity effects in vibration analysis of functionally graded beams were studied by using flexible boundary conditions [10]. Based on their study, the most critical factors affecting linear and non-linear frequencies are the percentage of porosity volume, boundary conditions, and the transition and rotational spring constants. A study was made using nanoplates that are FGP and resting on the foundation [11]. Porosity influence was considered by applying two-variable refined plates and Winkler-Pasternak elastic foundations. One of the main goals was to determine the relationship of the free vibration characteristics with elastic foundation stiffness, material properties, boundary conditions, and porosity.

The performance of porous beams with two distinct porosity distributions in terms of elastic buckling and bending was investigated by [12]. Transverse shear defor-

mation's impact was included using the Timoshenko beam theory. The Ritz technique was used to develop and then solve the algebraic governing equations. The modified couple stress theory was used by [13] to examine the FG microplate's forced vibration with porosity effects. Hamilton's principle and Navier type solution method was used to study FG beams with different thermal sinusoidal, loading, non–linear, linear, and uniform temperature field [14].

The modified couple stress theory was used by [13] to examine functionally graded microplates' forced vibration with porosity effects. Hamilton's principle and Navier type solution method was used to study functionally graded beams with a different type of thermal sinusoidal load non–linear, linear, and uniform temperature [14]. The transverse displacement and the non – dimensional frequencies were calculated by [15], and they demonstrated that these parameters increased with the increase of the porosity. Timoshenko beam theory, Lagrange equation method, and Ritz technique were used by [16] for free and forced vibration analysis of FG beam.

The finite element method is one of the most influential and efficient tools used for the numerical solution of a wide range of problems in structural mechanics [17–29]. Besides this, several researchers and engineers examine the dynamic response of structures [30–43]. Also, during the last decades, one of the most trend subjects in the research field is composite and FGP materials. For instance, some recent works [44–57] can be mentioned.

Literature survey shows that the free vibration response of sandwich FGP beam with the aid of ANSYS, which is a finite element package program the free vibration response of sandwich FGP beam with the aid of ANSYS, a finite element package program, has not been reported yet. This study aims to present benchmark free vibration characteristics for FGP sandwich beams. The sandwich beams are assumed to have a porous core and isotropic homogenous face sheets. Results are obtained for different values of porosity coefficients to investigate the impact of porosity on the free vibration characteristics. For the beam boundary conditions, clamped-clamped, clamped-hinged, hinged - hid clamped - free cases are considered four different cases. The shear deformation is taken into consideration in the analysis procedure. For porous material, the symmetric and uniform distributions are employed as two kinds of different distributions. To present this study better, it is ordered as follows: Section 2 gives the type of FGP materials and provides information about the details of the analysis. Section 3 shows the results and discussion, and finally, Section 4 is dedicated to the most important conclusion of this study.

2. MATERIALS AND METHOD

The finite element method is implemented to acquire the natural frequencies of the functionally graded po-
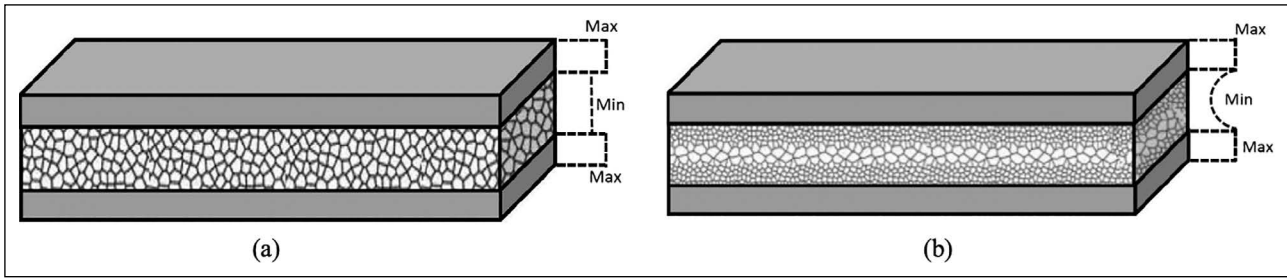
Figure 1. **(a)** FGP sandwich beam with uniform porosity distribution; **(b)** FGP sandwich beam with symmetric porosity distribution.

rous (FGP) sandwich beam shown in Figure 1, which has a length of L, a width of b, and a height of h. The beam has three layers in the thickness direction. The core layer is assumed to be FGP material and the top and the bottom layers are made up of isotropic homogenous material. In this paper two types of different FGP materials are used. The influence of the porosity coefficient for symmetric and uniform porosity distributions is investigated.

In this paper, Poisson's ratio is assumed to be constant. The variation of Young's modulus and mass density for the FGP sandwich beams are presented in this section. The material properties for the sandwich FGP beams are given in Eqs. (1–9) for uniform porosity distribution and in Eqs. (10–18) for symmetric porosity distribution [58].

Top Face $\left(+\dfrac{7h}{18} \leq z \leq +\dfrac{h}{2}\right)$
$$E(z) = E_1 \quad (1)$$
$$G(z) = G_1 \quad (2)$$
$$\rho(z) = \rho_1 \quad (3)$$

Core $\left(-\dfrac{7h}{18} \leq z \leq +\dfrac{7h}{18}\right)$
$$E(z) = E_1\,[\,1 - e_o\varphi\,] \quad (4)$$
$$G(z) = G_1\,[\,1 - e_o\varphi\,] \quad (5)$$
$$\rho(z) = \rho_1\sqrt{1 - e_o\varphi} \quad (6)$$

Bottom Face $\left(-\dfrac{h}{2} \leq z \leq -\dfrac{7h}{18}\right)$
$$E(z) = E_2 \quad (7)$$
$$G(z) = G_2 \quad (8)$$
$$\rho(z) = \rho_2 \quad (9)$$

Top Face $\left(+\dfrac{7h}{18} \leq z \leq +\dfrac{h}{2}\right)$
$$E(z) = E_1 \quad (10)$$
$$G(z) = G_1 \quad (11)$$
$$\rho(z) = \rho_1 \quad (12)$$

Core $\left(-\dfrac{7h}{18} \leq z \leq +\dfrac{7h}{18}\right)$
$$E(z) = E_1\left[1 - e_0 cos\left(\dfrac{\pi z}{h_c}\right)\right] \quad (13)$$
$$G(z) = G_1\left[1 - e_0 cos\left(\dfrac{\pi z}{h_c}\right)\right] \quad (14)$$
$$\rho(z) = \rho_1\left[1 - e_m cos\left(\dfrac{\pi z}{h_c}\right)\right] \quad (15)$$

Bottom Face $\left(-\dfrac{h}{2} \leq z \leq -\dfrac{7h}{18}\right)$
$$E(z) = E_2 \quad (16)$$
$$G(z) = G_2 \quad (17)$$
$$\rho(z) = \rho_2 \quad (18)$$

where h_c is the core thickness and constant φ is
$$\varphi = \dfrac{1}{e_o} - \dfrac{1}{e_o}\left(\dfrac{2}{\pi}\sqrt{1 - e_o} - \dfrac{2}{\pi} + 1\right)^2 \quad (19)$$

In the above equations, e_o is the porosity coefficient, h is the thickness of the cross-section, E_1, G_1 and ρ_1 are the maximum value for the modulus of elasticity, shear modulus, and mass density. The porosity coefficient for the mass density (e_m). Can be obtained by the following equation [3].
$$e_m = 1 - \sqrt{1 - e_0} \quad (20)$$

The solution procedure of the considered problem with the finite element package program ANSYS, BEAM 189, is implemented. This element has three nodes, each with six degrees of freedom. These degrees of freedom are directional displacement in x, y, and z directions and rotations about x, y, and z axes. BEAM189, a 3D element, is based on the first-order shear deformation theory. In this study, the in-plane free vibration characteristics are obtained. For this reason, the displacement in the y direction and rotations about the x and z axes are restrained. More detailed information about the theory of this element can be found in [59].

To generate the FGP sandwich beam model in Ansys Mechanical APDL [60], the material properties, such as mass density and Young's modulus, are first calculated based on the material functions. A data file is created in *.csv format for the calculated values. The section is divided into 36 layers in the thickness direction [3]. The cross-section mesh of the beam consists of 1296 elements, as seen in Figure 2. The first and last four layers are isotropic homogenous, and the middle layers are made up of functionally graded porous materials. Each material is defined to its specific layer using the Edit/ Built-up options of the Custom Sections in Ansys Mechanical APDL. For the mesh size, the beam is divided into 100 elements the longitudinal direction is divided into 100 elements in the longitudinal direction for the mesh size. It is worth to be mentioned that the mesh size is selected to obtain accurate mode shapes.
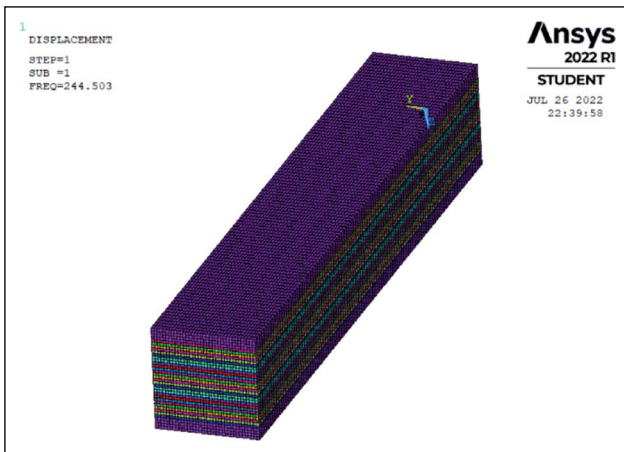
Figure 2. FGP sandwich beam finite element mesh.

3. NUMERICAL RESULTS AND DISCUSSION

The free vibration characteristics of the sandwich FGP beams are obtained for various values of porosity coefficients, two types of FG porosity distributions, and several boundary conditions. For the uniform porosity distribution, the musing modulus of elasticity is calculated using Eqs. (1–9). Eqs acquire the same material properties for the symmetric porosity distribution (10–18). The Poisson's ratio is taken as a constant value of 0.3. In this paper, the value of the maximum mass density ($\rho_1 = \rho_2$) is 7850 kg/m³, and

the value of the maximum modulus of elasticity ($E_1 = E_2$). It is considered 200 GPa for all tables and figures except Table 10. The program automatically calculates the maximum shear modulus with $\left(G_i = \frac{E_i}{2(1+v)}\right)$. The geometric properties of the beam are; h=0.5 m, b=0.5 m, and L=3 m.

The analysis methodology works on eighty-eight different FGP sandwich beams divided equally into two main groups depending on the symmetric and uniform porosity distribution. Each group differs in the type of supports of the beam and the porosity coefficients of FGP materials. All boundary conditions are listed in Table 1 related to rotation and directional displacements. In Table 1, '**i**' denotes the left end of the beam, while '**j**' stands for the right end of the beam.

As the first problem of this section, the symmetric porosity distribution is considered. Ten natural frequencies are calculated for various values of the porosity coefficient (e_0). Four types of boundary conditions are implemented. The free vibration characteristics values for the clamped–clamped supported beams are presented in Table 2.

By the same token, the free vibration characteristics are calculated for the C-H sandwich FGP beam with a core made up of symmetric porosity distribution. These results are determined using eleven different values of the porosity coefficient. Derived results are listed in Table 3.

A third example with the same approach will now be presented. In this part, a sandwich FGP beam of symmetry porosity will be handled with boundary conditions will be H-H. The computed free vibration frequencies are shown in Table 4.

Table 1. Beam boundary conditions

Type of the support	Boundary conditions	
	i	**j**
Clamped – Clamped (C-C)	Rotz = Roty = Rotx= Uz = Uy = Ux = 0	Rotz = Roty = Rotx= Uz = Uy = Ux = 0
Clamped – Hinged (C-H)	Rotz = Roty = Rotx= Uz = Uy = Ux = 0	Uz = Ux = Uy = 0
Hinged – Hinged (H-H)	Uz = Ux = Uy = 0	Uz = Ux = Uy = 0
Clamped – Free (C-F)	Rotz = Roty = Rotx= Uz = Uy = Ux = 0	-----

Table 2. Natural frequencies of C-C supported FGP sandwich beam with symmetric porosity distribution (Hz)

Mode	e_0										
	0.1	0.2	0.25	0.3	0.4	0.5	0.6	0.7	0.75	0.8	0.9
1	244.50	243.56	243.08	242.45	241.16	239.26	236.76	232.84	230.05	226.01	210.86
2	576.28	570.34	567.17	563.46	555.39	544.95	531.75	513.04	500.55	483.83	424.91
3	976.87	820.98	816.18	810.87	801.33	791.39	782.69	775.27	772.89	770.75	669.90
4	1412.10	962.89	955.43	946.93	928.41	905.33	876.86	838.02	812.87	780.16	754.70
5	1868.90	1387.90	1375.00	1360.50	1328.90	1290.00	1242.10	1176.30	1131.50	1065.70	774.01
6	2337.20	1642.00	1632.40	1621.70	1602.70	1582.80	1565.40	1526.10	1378.80	1216.00	955.65
7	2811.10	1833.40	1814.40	1793.30	1747.10	1690.90	1621.80	1537.70	1459.50	1361.40	1001.40
8	3076.50	2288.80	2262.70	2233.50	2167.20	2063.50	1835.30	1550.50	1545.80	1541.50	1247.20
9	3302.80	2462.90	2448.50	2432.60	2399.20	2169.70	2031.70	1858.70	1699.60	1541.60	1285.60
10	3446.80	2748.20	2713.90	2636.90	2404.00	2374.20	2161.30	1902.80	1819.10	1701.20	1542.20

Table 3. Natural frequencies of C-H supported FGP sandwich beam with symmetric porosity distribution (Hz)

Mode	e_0										
	0.1	0.2	0.25	0.3	0.4	0.5	0.6	0.7	0.75	0.8	0.9
1	179.65	179.48	179.43	179.29	179.09	178.58	177.85	176.39	175.20	173.23	164.45
2	507.71	503.99	502.03	499.65	494.52	487.62	478.72	465.63	456.67	444.35	399.97
3	916.88	820.98	816.18	810.87	801.33	791.39	782.69	775.27	772.89	752.71	646.50
4	1366.80	905.77	899.83	893.00	878.09	859.18	835.57	802.76	781.21	770.75	694.45
5	1837.50	1345.70	1334.40	1321.70	1294.00	1259.70	1217.60	1160.20	1122.40	1065.60	774.01
6	2318.50	1642.00	1632.40	1621.70	1602.70	1582.80	1565.40	1438.70	1275.90	1105.90	866.61
7	2802.50	1804.90	1787.60	1768.10	1725.70	1673.80	1609.60	1526.10	1454.40	1312.60	958.07
8	2980.30	2273.30	2249.20	2222.20	2162.60	2025.10	1750.60	1550.50	1534.90	1427.40	1139.70
9	3231.70	2462.90	2448.50	2432.60	2289.30	2094.10	1969.00	1683.90	1545.80	1541.50	1248.60
10	3308.70	2737.30	2646.60	2531.50	2404.00	2283.00	2042.40	1902.50	1806.10	1641.10	1431.30

Table 4. Natural frequencies of H-H supported FGP sandwich beam with symmetric porosity distribution (Hz)

Mode	e_0										
	0.1	0.2	0.25	0.3	0.4	0.5	0.6	0.7	0.75	0.8	0.9
1	121.88	122.16	122.34	122.49	122.93	123.30	123.73	124.03	124.07	124.25	124.66
2	435.07	433.30	432.39	431.20	428.70	425.01	420.05	412.16	406.48	398.21	366.36
3	852.41	820.98	816.18	810.87	801.33	791.39	782.69	764.77	747.39	724.15	644.76
4	1318.00	844.26	839.91	834.81	823.69	809.21	790.87	775.27	772.89	770.75	650.26
5	1804.30	1300.10	1290.60	1279.80	1256.10	1226.50	1190.10	1140.50	1108.60	1061.30	772.59
6	2298.60	1642.00	1632.40	1621.70	1602.70	1582.80	1565.40	1406.00	1240.40	1067.30	774.01
7	2795.00	1774.90	1759.20	1741.60	1703.30	1656.50	1599.70	1524.30	1371.50	1190.30	933.68
8	2943.40	2256.60	2234.30	2209.40	2155.40	1992.20	1714.20	1538.50	1476.70	1416.40	1021.50
9	3085.10	2462.90	2448.50	2432.60	2252.30	2090.40	1849.20	1550.50	1545.80	1480.20	1226.60
10	3290.80	2725.50	2612.80	2496.20	2390.60	2129.00	2012.30	1851.90	1674.50	1541.50	1306.00

Table 5. Natural frequencies of C-F supported FGP sandwich beam with symmetric porosity distribution (Hz)

Mode	e_0										
	0.1	0.2	0.25	0.3	0.4	0.5	0.6	0.7	0.75	0.8	0.9
1	44.48	44.65	44.76	44.87	45.14	45.42	45.79	46.20	46.44	46.63	46.75
2	247.68	246.81	246.36	245.75	244.46	242.46	239.67	235.01	231.52	226.30	204.98
3	604.92	410.49	408.09	405.43	400.66	395.69	391.34	387.63	386.44	385.37	387.00
4	1025.20	599.22	596.14	592.52	584.53	573.97	560.31	540.38	526.80	508.38	443.50
5	1479.10	1010.70	1002.80	993.86	974.02	948.83	916.92	871.79	841.45	800.66	647.33
6	1945.90	1231.50	1224.30	1216.30	1202.00	1187.10	1174.00	1162.90	1159.30	1094.80	808.05
7	2413.00	1453.30	1439.30	1423.60	1388.90	1345.50	1291.10	1214.90	1163.70	1156.10	876.53
8	2846.30	1906.20	1884.70	1860.40	1806.00	1736.30	1639.70	1465.50	1333.30	1177.20	1092.50
9	3095.90	2052.40	2040.40	2027.20	2003.30	1978.50	1862.80	1631.80	1529.50	1414.10	1148.70
10	3239.80	2356.20	2324.80	2289.10	2205.40	2080.20	1956.70	1755.30	1627.50	1486.40	1161.00

In the last case of the symmetry porosity distribution, we seek to determine the natural frequencies of an FGP sandwich beam that is exposed to C-F boundary conditions. The frequencies of the current case are tabled in Table 5.

The same procedure employed for the symmetry porosity distribution will be implemented to acquire the natural frequencies of the FGP sandwich beams with a uniform porosity distribution core. We now turn on to study the ef-

Table 6. Natural frequencies of C-C supported FGP sandwich beam with uniform porosity distribution (Hz)

Mode	e_0										
	0.1	0.2	0.25	0.3	0.4	0.5	0.6	0.7	0.75	0.8	0.9
1	243.76	242.11	241.25	240.36	238.49	236.43	234.12	231.40	229.79	227.92	222.62
2	576.21	570.54	567.54	564.39	557.59	549.94	541.06	530.28	523.79	516.19	494.72
3	830.58	819.33	813.46	807.41	794.71	781.06	766.23	749.86	740.93	731.34	709.33
4	978.59	967.07	960.93	954.49	940.54	924.76	906.41	884.18	870.86	855.33	812.27
5	1416.40	1397.80	1387.90	1377.50	1354.90	1329.30	1299.60	1263.60	1242.10	1217.10	1148.00
6	1661.20	1638.70	1626.90	1614.80	1589.40	1562.10	1532.50	1499.70	1481.90	1462.70	1418.70
7	1876.40	1850.00	1835.90	1821.20	1789.10	1752.80	1710.60	1659.60	1629.20	1593.90	1497.00
8	2348.30	2313.50	2294.90	2275.30	2232.80	2184.40	2127.70	2057.70	2013.80	1956.70	1709.50
9	2491.70	2458.00	2440.40	2422.20	2384.10	2343.20	2298.70	2249.60	2181.70	2066.30	1871.00
10	2826.50	2782.70	2759.20	2734.50	2680.50	2618.80	2485.50	2290.80	2222.80	2194.00	2033.10

Table 7. Natural frequencies of C-H supported FGP sandwich beam with uniform porosity distribution (Hz)

Mode	e_0										
	0.1	0.2	0.25	0.3	0.4	0.5	0.6	0.7	0.75	0.8	0.9
1	178.87	177.93	177.45	176.96	175.96	174.91	173.78	172.53	171.82	171.03	168.86
2	506.99	502.80	500.59	498.28	493.36	487.87	481.58	474.04	469.53	464.27	449.42
3	830.58	819.33	813.46	807.41	794.71	781.06	766.23	749.86	740.93	731.34	709.33
4	917.62	907.90	902.73	897.32	885.64	872.47	857.21	838.75	827.70	814.80	778.85
5	1370.00	1353.20	1344.30	1334.90	1314.70	1291.70	1265.10	1232.90	1213.70	1191.30	1129.40
6	1661.20	1638.70	1626.90	1614.80	1589.40	1562.10	1532.50	1499.70	1481.90	1462.70	1418.70
7	1843.80	1819.10	1805.90	1792.10	1762.10	1728.20	1688.70	1641.00	1612.60	1579.40	1487.80
8	2328.30	2295.10	2277.30	2258.60	2218.10	2172.20	2118.70	2053.60	2013.20	1937.00	1622.90
9	2491.70	2458.00	2440.40	2422.20	2384.10	2343.20	2298.70	2183.40	2071.40	1975.50	1831.80
10	2816.60	2774.00	2751.20	2727.00	2671.70	2550.90	2381.10	2249.60	2222.80	2193.00	1893.80

Table 8. Natural frequencies of H-H supported FGP sandwich beam with uniform porosity distribution (Hz)

Mode	e_0										
	0.1	0.2	0.25	0.3	0.4	0.5	0.6	0.7	0.75	0.8	0.9
1	121.19	120.75	120.53	120.31	119.90	119.52	119.18	118.90	118.80	118.73	118.72
2	433.84	430.98	429.50	427.96	424.74	421.23	417.32	412.77	410.11	407.03	398.47
3	830.58	819.33	813.46	807.41	794.71	781.06	766.23	749.86	740.93	731.34	709.33
4	852.17	844.31	840.14	835.80	826.47	816.03	804.02	789.58	780.95	770.89	742.74
5	1320.00	1305.20	1297.30	1289.10	1271.20	1251.10	1227.80	1199.60	1182.80	1163.10	1108.70
6	1661.20	1638.70	1626.90	1614.80	1589.40	1562.10	1532.50	1499.70	1481.90	1462.70	1418.70
7	1809.40	1786.50	1774.20	1761.40	1733.60	1702.30	1665.80	1621.80	1595.50	1564.90	1480.80
8	2307.10	2275.50	2258.60	2240.80	2202.30	2158.80	2108.30	2047.30	2010.90	1906.00	1586.50
9	2491.70	2458.00	2440.40	2422.20	2384.10	2343.20	2298.70	2146.90	2033.10	1968.70	1722.40
10	2807.10	2766.40	2744.60	2721.70	2668.80	2517.10	2345.70	2249.60	2169.90	2042.50	1853.20

fects of the porosity on the outcomes of the free vibration analysis of these structures. The examples deal with calculating the natural frequencies of C-C, C-H, H-H, and C-F supported FGP sandwich beams. Each case's first to tenth natural frequencies are calculated for several porosity coefficient values and summarized in Tables 6–9.

Table 9. Natural Frequencies of C-F supported FGP sandwich beam with uniform porosity distribution (Hz)

Mode	e_0										
	0.1	0.2	0.25	0.3	0.4	0.5	0.6	0.7	0.75	0.8	0.9
1	44.20	44.07	44.00	43.95	43.84	43.76	43.71	43.71	43.74	43.80	44.07
2	246.92	245.37	244.56	243.73	241.99	240.10	238.00	235.55	234.12	232.46	227.75
3	415.29	409.67	406.73	403.71	397.35	390.53	383.11	374.93	370.46	365.67	354.66
4	604.73	599.25	596.35	593.33	586.83	579.55	571.16	561.05	554.99	547.91	527.98
5	1027.20	1015.50	1009.30	1002.80	988.79	972.91	954.43	931.99	918.51	902.73	858.50
6	1245.90	1229.00	1220.20	1211.10	1192.10	1171.60	1149.30	1124.80	1111.40	1097.00	1064.00
7	1484.20	1465.10	1454.80	1444.10	1420.70	1394.30	1363.50	1326.00	1303.40	1277.10	1203.30
8	1955.20	1927.30	1912.30	1896.60	1862.40	1823.30	1777.40	1720.80	1686.20	1645.00	1520.10
9	2076.50	2048.30	2033.70	2018.50	1986.80	1952.60	1915.60	1874.70	1852.30	1828.40	1728.20
10	2427.90	2390.00	2369.60	2348.10	2300.90	2246.40	2181.10	2097.50	2043.20	1972.10	1773.30

Table 10. Natural frequencies of C-C supported FGP unsymmetrical sandwich beam with uniform porosity distribution (Hz)

Mode	e_0										
	0.1	0.2	0.25	0.3	0.4	0.5	0.6	0.7	0.75	0.8	0.9
1	232.5	230.51	229.47	228.4	226.15	223.71	221.01	217.94	216.19	214.22	209.06
2	557.66	551.66	548.49	545.19	538.15	530.35	521.49	511.04	504.92	497.9	478.92
3	830.03	817.81	811.4	804.78	790.78	775.6	758.91	740.2	729.83	718.54	691.82
4	956.25	944.53	938.32	931.84	917.93	902.4	884.64	863.57	851.17	836.91	798.43
5	1393.5	1375	1365.1	1354.8	1332.7	1307.9	1279.4	1245.6	1225.7	1202.8	1141
6	1660.1	1635.6	1622.8	1609.6	1581.6	1551.2	1517.8	1480.4	1459.7	1437.1	1383.6
7	1854.8	1828.7	1814.9	1800.4	1769.2	1734.2	1694	1646.1	1618	1585.6	1498.4
8	2330.1	2296	2277.9	2258.9	2217.9	2172	2119.1	2056	2018.7	1975.8	1858.2
9	2490.1	2453.4	2434.2	2414.3	2372.4	2326.8	2276.7	2220.6	2189.5	2155.6	2075.5
10	2813.5	2771	2748.4	2724.7	2673.5	2615.9	2549.6	2470.3	2423.2	2368.6	2078.5

To extend the solutions procedure to unsymmetrical beams as well. The sandwich beam is considered with a steel top face, an FGP core with uniform distribution, and an aluminum bottom face. In this part, the value of the mass density (ρ_2). Are 2700 kg/m³, and the value of the modulus of elasticity (E_2) It is considered to be 70 GPa. Results are obtained and compared for clamped – clamped supported beam in Table 10. The geometric properties are the same as in the previous example.

The above Tables 2–10 demonstrate some essential ingredients of the free vibration response of FGP sandwich beams. It is visible to see the influence of the porosity coefficient on the natural frequencies from the given comparisons. In each of the above examples, we dealt with 11 different values of e_0. When the uniform distribution was implemented, the natural frequencies showed an apparent decrease, with porosity coefficients increasing for all analyzed beams. Also, for the symmetric porosity distribution, it is carried out that for C-C and C-H, the natural frequencies decrease when the porosity coefficient increases. When H-H and C-F boundary conditions are used, it seems that the first natural frequencies increase while the remaining frequencies decrease. From the general review of analysis, the calculated results demonstrate good compatibility with expected beam behavior. It should also be emphasized that boundary conditions considerably affect the natural frequencies of the FGP sandwich beams. As might well be expected, the highest values of the natural frequencies are in C-C, and the lowest values of the free vibration characteristics are in C-F boundary conditions. To further discuss the finite element procedure for the free vibration response of the problem at hand, PLANE183 is also utilized. Results are obtained for uniform porosity distribution. Calculated results are listed in Table 11 for clamped-clamped supported beams.

When Table 6 and Table 11 are compared, it can be seen that the results of both finite element types are in good agreement. The slight difference is because of differences in the assumptions and theory of the elements.

Table 11. Natural frequencies of C-C supported FGP sandwich beam with uniform porosity distribution obtained with PLANE183 (Hz)

Mode	e_0										
	0.1	**0.2**	**0.25**	**0.3**	**0.4**	**0.5**	**0.6**	**0.7**	**0.75**	**0.8**	**0.9**
1	245.49	243.95	243.15	242.32	240.57	238.67	236.53	234.02	232.54	230.81	225.89
2	582.42	577.2	574.43	571.53	565.31	558.31	550.22	540.43	534.54	527.64	508.13
3	833.3	822.07	816.22	810.18	797.5	783.87	769.05	752.68	743.73	734.12	711.93
4	992.31	981.75	976.13	970.24	957.52	943.17	926.51	906.34	894.25	880.14	840.84
5	1440.3	1423.3	1414.3	1404.8	1384.2	1361	1334.1	1301.4	1281.9	1259.2	1196.2
6	1661.3	1638.6	1626.7	1614.5	1588.8	1561	1530.8	1497.1	1478.5	1458.4	1411.1
7	1912.3	1888.2	1875.4	1861.9	1832.7	1799.6	1761.2	1714.6	1686.8	1654.3	1564.8
8	2397.6	2365.8	2348.8	2331	2292.2	2248.3	2197.2	2135.2	2098	2054.8	1935.6
9	2475	2440.2	2421.9	2403	2363	2319.7	2271.8	2217.7	2187.3	2153.8	2071
10	2889.7	2849.7	2828.3	2805.8	2756.9	2701.5	2636.9	2558.6	2511.8	2427.3	2207
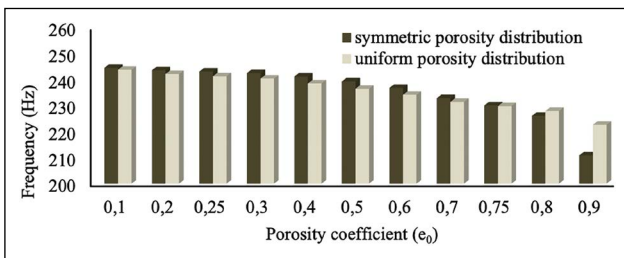
Figure 3. Comparison of the first natural frequencies for C-C sandwich FGP beam.
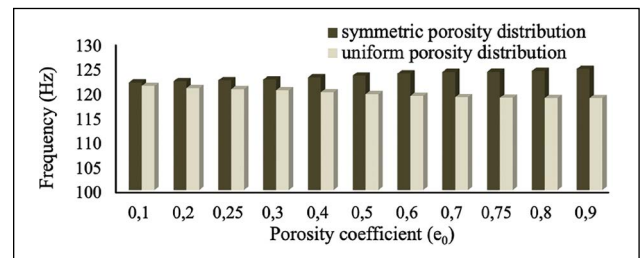
Figure 5. Comparison of the first natural frequencies for H-H sandwich FGP beam.
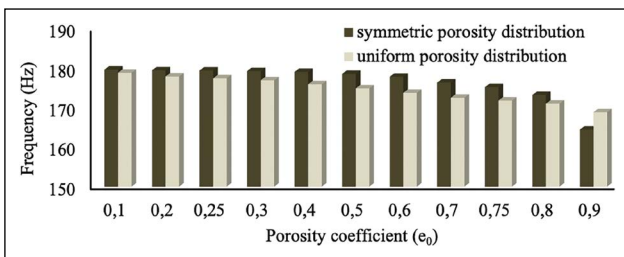
**Figure 4**. Comparison of the first natural frequencies for C-H sandwich FGP beam.
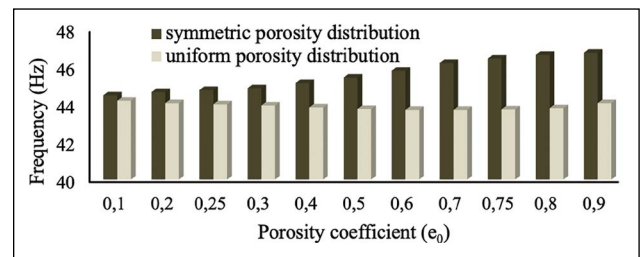
Figure 6. Comparison of the first natural frequencies for C-F sandwich FGP beam.

One of our objectives in this section is to discuss the difference in the influence of the symmetric and uniform distribution on the free vibration sandwich FGP beams. For this reason, the following Figures 3–6 are illustrated to compare the effect of two types of porous distribution on the free vibration response of the considered structures.

As can be seen in Figures 3–6, the material distribution of the core has an essential effect on the structure's natural frequencies. Figure 3 shows that the first natural frequencies are higher in symmetric porosity distribution for values of e_0 less than 0.8 when implementing C-C boundary conditions. Figure 4 demonstrates that when the beam is C-H, the first natural frequencies are higher in uniform porosity distribution for values of e_0 more than 0.9. It is apparent in

Figures 5–6 that values of the symmetric porosity distribution are greater than those of the uniform porosity distribution when the beam is H-H and C-F.

4. CONCLUSIONS

In this study, the free vibration response of FGP sandwich beams is investigated with the aid of the finite element method. The first-order shear deformation theory is used. Two kinds of different porous materials are considered for the core of the sandwich structure. The influence of the porosity coefficient and boundary conditions on the natural frequencies is investigated, and the following results can be concluded.

- When the uniform porous material is used in the core of the sandwich beam, an inversely proportional relationship between porosity and frequency is observed, which means higher frequency recorded was for lower porosity coefficients.
- For the symmetric porous material in the core of the beam, it is carried out that C-C and C-H, the free vibration characteristic values decrease when the porosity coefficient increases. When H-H and C-F boundary conditions are used, the first natural frequencies increase, and the other frequencies decrease.
- Higher frequencies were recorded at C-C beams, and lower frequencies were recorded at C-F beams.
- The type of porosity distribution is essential for the value of the free vibration characteristics.
- For H-H and C-F boundary conditions, the natural frequencies of the FGP sandwich beam are greater in symmetric porosity distributions than those of the uniform porosity distribution.
- For C-C and C-H, when the value of e_0 is more than 0.8, the natural frequencies in FGP sandwich beams with uniform porosity distributions start to get higher than those of the symmetric porosity distribution.

ETHICS

There are no ethical issues with the publication of this manuscript.

DATA AVAILABILITY STATEMENT

The authors confirm that the data that supports the findings of this study are available within the article. Raw data that support the finding of this study are available from the corresponding author, upon reasonable request.

CONFLICT OF INTEREST

The authors declare that they have no conflict of interest.

FINANCIAL DISCLOSURE

The authors declared that this study has received no financial support.

PEER-REVIEW

Externally peer-reviewed.

REFERENCES

[1]   Prasad, M. S., Reddy, P. S., Manoj, M., & Murthy, N. G. (2014). Analysis of sandwich beam. *International Journal of Science Engineering and Advance Technology*, 2(12), 901–908.

[2]   Wu, H., Yang, J., & Kitipornchai, S. (2020). Mechanical analysis of functionally graded porous structures: A review. *International Journal of Structural Stability and Dynamics*, 20(13), Article 2041015. [CrossRef]

[3]   Noori, A. R., Aslan, T. A., & Temel, B. (2021). dynamic analysis of functionally graded porous beams using complementary functions method in the Laplace domain. *Composite Structures*, 256, Article 113094. [CrossRef]

[4]   Zhao, J., Wang, Q., Deng, X., Choe, K., Xie, F., & Shuai, C. (2018). A modified series solution for free vibration analyses of moderately thick functionally graded porous (FGP) deep curved and straight beams. *Composites Part B: Engineering*, 165, 155–166. [CrossRef]

[5]   Akbaş, Ş. D. (2017). Forced vibration analysis of functionally graded porous deep beams. *Composite Structures*, 186, 293–302. [CrossRef]

[6]   Rao, S. S. (2007). *Vibration of continuous systems.* John Wiely & Sons.

[7]   Wang, Q., & Quek, S. T. (2000). Flexural vibration analysis of sandwich beam coupled with piezoelectric actuator. *Smart Materials and Structures*, 9(1), Article 103. [CrossRef]

[8]   Chen, D., Kitipornchai, S., & Yang, J. (2016). Nonlinear free vibration of shear deformable sandwich beam with a functionally graded porous core. *Thin-Walled Structures*, 107, 39–48. [CrossRef]

[9]   Yang, Y., Lam, C. C., Kou, K. P., & Iu, V. P. (2014). Free vibration analysis of the functionally graded sandwich beams by a mesh free boundary-domain integral equation method. *Composite Structures*, 117, 32–39. [CrossRef]

[10]   Wattanasakulpong, N., & Ungbhakorn, V. (2014). Linear and nonlinear vibration analysis of elastically restrained ends FGM beams with porosities. *Aerospace Science and Technology*, 32(1), 111–120. [CrossRef]

[11]   Mechab, I., Mechab, B., Benaissa, S., Serier, B., & Bouiadjra, B. B. (2016). Free vibration analysis of FGM nanoplate with porosities resting on Winkler Pasternak elastic foundations based on two-variable refined plate theories. *Journal of the Brazilian Society of Mechanical Sciences and Engineering*, 38(8), 2193–2211. [CrossRef]

[12]   Chen, D., Yang, J., & Kitipornchai, S. (2015). Elastic buckling and static bending of shear deformable functionally graded porous beam. *Composite Structures*, 33, 54–61. [CrossRef]

[13]   Şimşek, M., & Aydın, M. (2016). Size-dependent forced vibration of an imperfect functionally graded (FG) microplate with porosities subjected to a moving load using the modified couple stress theory *Composite Structures*, 160, 408–421. [CrossRef]

[14]   Ebrahimi, F., & Jafari, A. (2016). A higher-order thermomechanical vibration analysis of temperature-dependent FGM beams with porosities. *Journal of Engineering*, 2016, Article 9561504. [CrossRef]

[15]   Ait Atmane, H., Tounsi, A., & Bernard, F. (2015). Effect of thickness stretching and porosity on mechani-

cal response of a functionally graded beams resting on elastic foundations. *International Journal of Mechanics and Materials in Design*, 13(1), 71–84. [CrossRef]

[16] Chen, D., Yang, J., & Kitipornchai, S. (2016). Free and forced vibrations of shear deformable functionally graded porous beams. *International Journal of Mechanical Sciences*, 108, 14–22. [CrossRef]

[17] Dilbas, H. (2021). Application of finite element method on recycled aggregate concrete and reinforced recycled aggregate concrete: A review. *Journal of Sustainable Construction Materials and Technologies*, 4(6), 173–191. [CrossRef]

[18] Doori, S., & Noori, A. R. (2021). Finite element approach for the bending analysis of castellated steel beams with various web openings. *ALKU Journal of Science*, 2(3), 38–49. [CrossRef]

[19] Noori, A. R., Aslan, T. A., & Temel, B. (2019). Dairesel plakların sonlu elemanlar yöntemi ile laplace uzayında dinamik analizi. *Omer Halisdemir University Journal of Engineering Sciences*, 8(1), 193–205. [CrossRef]

[20] Aslan, T. A., & Temel, B. (2022). Finite element analysis of the seepage problem in the dam body and foundation based on the Galerkin's approach. *European Mechanical Science*, 6(2), 143–151. [CrossRef]

[21] Yildirim, S. (2021). Free vibration of axially or transversely graded beams using finite-element and artificial intelligence. *Alexandria Engineering Journal*, 6, 2220–2229. [CrossRef]

[22] Temel, B., & Şahan, M. F. (2013). Transient analysis of orthotropic, viscoelastic thick plates in the Laplace domain. *European Journal of Mechanics A/ Solids*, 37, 96–105. [CrossRef]

[23] Aribas, U. N., Ermis, M., Eratli, N., & Omurtag, M. H. (2019). The static and dynamic analyses of warping included composite exact conical helix by mixed FEM. *Composites Part B*, 160, 285–297. [CrossRef]

[24] Chen, J., Shou, Y., & Zhou, X. (2022). Implementation of the novel perfectly matched layer element for elastodynamic problems in time-domain finite element method. *Soil Dynamics and Earthquake Engineering*, 152, Article 107054. [CrossRef]

[25] Hobiny, A. D., & Abbas, I. (2022). The impacts of variable thermal conductivity in a semiconducting medium using finite element method. *Case Studies in Thermal Engineering*, 31, Article 101773. [CrossRef]

[26] Chai, Y., Li, W., & Liu, Z. (2022). Analysis of transient wave propagation dynamics using the enriched finite element method with interpolation cover functions. *Applied Mathematics and Computation*, 412, Article 126564. [CrossRef]

[27] Wu, N., Liang, Z., Zhang, Z., Li, S., & Lang, Y. (2022). Development and verification of three-dimensional equivalent discrete fracture network modelling based on the finite element method. *Engineering Geology*, 306, Article 106759. [CrossRef]

[28] Zhou, L., Wang, J., Liu, M., Li, M., & Chai, Y. (2022). Evaluation of the transient performance of magneto-to-electro-elastic based structures with the enriched finite element method. *Composite Structures*, 280, Article 114888. [CrossRef]

[29] Noori, A. R., & Temel, B. (2020). On the vibration analysis of laminated composite parabolic arches with variable cross-section of various ply stacking sequences. *Mechanics of Advanced Materials and Structures*, 27(19), 1658–1672. [CrossRef]

[30] Van Vinh, P. (2022). Nonlocal free vibration characteristics of power-law and sigmoid functionally graded nanoplates considering variable nonlocal parameter. *Physica E: Low-dimensional Systems and Nanostructures*, 135, Article 114951. [CrossRef]

[31] Akbari, H., Azadi, M., & Fahham, H. (2022). Free vibration analysis of thick sandwich cylindrical panels with saturated FG-porous core. *Mechanics Based Design of Structures and Machines*, 50(4), 1268–1286. [CrossRef]

[32] Liu, X., Zhao, Y., Zhou, W., & Banerjee, J. R. (2022). Dynamic stiffness method for exact longitudinal free vibration of rods and trusses using simple and advanced theories. *Applied Mathematical Modelling*, 104, 401–420. [CrossRef]

[33] Daikh, A. A., Bachiri, A., Houari, M. S. A., & Tounsi, A. (2022). Size dependent free vibration and buckling of multilayered carbon nanotubes reinforced composite nanoplates in thermal environment. *Mechanics Based Design of Structures and Machines*, 50(4), 1371–1399. [CrossRef]

[34] Chen, W., Luo, W. M., Chen, S. Y., & Peng, L. X. (2022). A FSDT meshfree method for free vibration analysis of arbitrary laminated composite shells and spatial structures. *Composite Structures*, 279, Article 114763. [CrossRef]

[35] Garg, A., Chalak, H. D., Zenkour, A. M., Belarbi, M. O., & Sahoo, R. (2022). Bending and free vibration analysis of symmetric and unsymmetric functionally graded CNT reinforced sandwich beams containing softcore. *Thin-Walled Structures*, 170, Article 108626. [CrossRef]

[36] Rachid, A., Ouinas, D., Lousdad, A., Zaoui, F. Z., Achour, B., Gasmi, H., Butt T.A. & Tounsi, A. (2022). Mechanical behavior and free vibration analysis of FG doubly curved shells on elastic foundation via a new modified displacements field model of 2D and quasi-3D HSDTs. *Thin-Walled Structures*, 172, Article 108783. [CrossRef]

[37] Bozyigit, B., & Acikgoz, S. (2022). Determination of free vibration properties of masonry arch bridges using the dynamic stiffness method. *Engineering Structures*, 250, Article 113417. [CrossRef]

[38] Babuscu Yesil, U., & Yahnioglu, N. (2022). Free vibration of simply supported piezoelectric plates containing a cylindrical cavity. *Archive of Applied Mechanics*, 92, 2665–2678. [CrossRef]

[39] Jin, H., Sui, S., Zhu, C., & Li, C. (2022). Axial free vibration of rotating fg piezoelectric nano rods accounting for nonlocal and strain gradient effects. *Journal of Vibration Engineering & Technologies*, 1–13. [CrossRef]

[40] Zamani, H. A. (2021). Free vibration of functionally graded viscoelastic foam plates using shear- and normal-deformation theories. *Mechanics of Time-Dependent Materials*, 1–22. [CrossRef]

[41] Yildirim, S. (2020). An efficient method for the plane vibration analysis of composite sandwich beam with an orthotropic core. *Cumhuriyet Science Journal*, 41(2), 521–526. [CrossRef]

[42] Temel, B. (2004). Transient analysis of viscoelastic helical rods subject to time-dependent loads. *International Journal of Solids and Structures*, 41(5–6), 1605–1624. [CrossRef]

[43] Calim, F. F. (2016). Free and forced vibration analysis of axially functionally graded Timoshenko beams on two-parameter viscoelastic foundation. *Composites Part B*, 103, 98–112. [CrossRef]

[44] Noori, A. R. , Rasooli, H. , Aslan, T. A. & Temel, B. (2020). Static analysis of functionally graded sandwich beams by the complementary functions method. *Çukurova University Journal of the Faculty of Engineering and Architecture*, 35(4), 1091–1102.

[45] Rasooli, H., Noori, A. R., & Temel, B. (2021). On the static analysis of laminated composite frames having variable cross section. *Journal of the Brazilian Society of Mechanical Sciences and Engineering*, 43, Article 258. [CrossRef]

[46] Humaish, H., Ruet, B., Marmoret, L., & Beji, H. (2016). Assessment of long time approximation equation to determine thermal conductivity of high porous materials with NSS probe. *Journal of Sustainable Construction Materials and Technologies*, 1(1), 1–15. [CrossRef]

[47] Pham, Q. H., Tran, T. T., Tran, V. K., Nguyen, P. C., & Nguyen-Thoi, T. (2022). Free vibration of functionally graded porous non-uniform thickness annular-nanoplates resting on elastic foundation using ES-MITC3 element. *Alexandria Engineering Journal*, 61, 1788–1802. [CrossRef]

[48] Zghal, S., Ataoui, D., & Dammak, F. (2022). Static bending analysis of beams made of functionally graded porous materials. *Mechanics Based Design of Structures and Machines*, 50(3), 1012–1029. [CrossRef]

[49] Chen, D., Rezaei, S., Rosendahl, P. L., Xu, B. X., & Schneider, J. (2022). Multiscale modelling of functionally graded porous beams: Buckling and vibration analyses. *Engineering Structures*, 266, Article 114568. [CrossRef]

[50] Najibi, A., & Shojaeefard, M. H. (2022). Fourier and time-phase-lag heat conduction analysis of the functionally graded porosity media. *International Communications in Heat and Mass Transfer*, 136, Article 106183. [CrossRef]

[51] Ramteke, P. M., Panda, S. K., & Patel, B. (2022). Nonlinear eigenfrequency characteristics of multi-directional functionally graded porous panels. *Composite Structures*, 279, Article 114707. [CrossRef]

[52] Liu, Y., Qin, Z., & Chu, F. (2022). Analytical study of the impact response of shear deformable sandwich cylindrical shell with a functionally graded porous core. *Mechanics of Advanced Materials and Structures*, 29(9), 1338–1347. [CrossRef]

[53] Surmeneva, M. A., Khrapov, D., Prosolov, K., Kozadayeva, M., Koptyug, A., Volkova, A., Paveleva, A. & Surmenev, R. A (2022). The influence of chemical etching on porous structure and mechanical properties of the Ti6AL4V Functionally Graded Porous Scaffolds fabricated by EBM. *Materials Chemistry and Physics*, 275, Article 125217. [CrossRef]

[54] Ansari, R., Oskouie, M. F., & Zargar, M. (2022). Hygrothermally induced vibration analysis of bidirectional functionally graded porous beams. *Transport in Porous Media*, 142, 41–62. [CrossRef]

[55] Teng, M. W., & Wang, Y. Q. (2021). Nonlinear forced vibration of simply supported functionally graded porous nanocomposite thin plates reinforced with graphene platelets. *Thin-Walled Structures*, 164, Article 107799. [CrossRef]

[56] Pham, Q. H., Tran, T. T., Tran, V. K., Nguyen, P. C., Nguyen-Thoi, T., & Zenkour, A. M. (2021). Bending and hygro-thermo-mechanical vibration analysis of a functionally graded porous sandwich nanoshell resting on elastic foundation. *Mechanics of Advanced Materials and Structures*, 1–21. [CrossRef]

[57] Su, J., Qu, Y., Zhang, K., Zhang, Q., & Tian, Y. (2021). Vibration analysis of functionally graded porous piezoelectric deep curved beams resting on discrete elastic supports. *Thin-Walled Structures*, 164, Article 107838. [CrossRef]

[58] Wattanasakulpong, N., & Eiadtrong, S. (2022). Transient responses of sandwich plates with a functionally graded porous core: Jacobi-Ritz method. International *Journal of Structural Stability and Dynamics*, [Epub ahead of print] doi: 10.1142/S0219455423500396 [CrossRef]

[59] ANSYS Mechanical APDL Element Reference. *Mechanical APDL element reference*. Pennsylvania: ANSYS Inc; 2013.

[60] ANSYS Inc. (Oct 10, 2022). *Gain greater engineering and product life cycle perspectives 2022 product releases & updates*. Release Ansys 2022 R2, Canonsburg, PA, 2022. Available at: https://www.ansys.com/products/release-highlights